

Influence of Gas-Liquid Separator Design on Performance of Airlift Bioreactors

Mateus N. Esperança, Marcel O. Cerri, Alberto C. Badino

Abstract—The performance of airlift bioreactors are closely related with their geometry, especially the gas-liquid separator design. In this study, the influence of the gas-liquid separator geometry on oxygen transfer and gas hold-up was evaluated in 10-L concentric-tube airlift bioreactor operating with distilled water and xanthan gum solution. The specific airflow rate (ϕ_{AIR}) exhibited the higher effect on the oxygen transfer coefficient (k_La) for both fluids. While the gas-liquid separator openness angle (α) and liquid volume fraction on the gas-liquid separator (V_{GLS}) have presented opposite effects on oxygen mass transfer, they affected negatively the global gas hold-up of distilled water system. The best degassing zone geometry corresponded to a 90° openness angle with 10% of the liquid on it.

Keywords—Airlift bioreactor, gas holdup, gas-liquid separator, oxygen transfer.

I. INTRODUCTION

AIRLIFT bioreactors have been becoming an excellent alternative to conventional stirred tank reactors (*STR*) in chemical and biochemical processes [1], [2], due to its characteristics such as cheap and simple construction and operation, absence of mechanical stirrer, good heat and mass transfer, and low energy costs [2], [3]. These equipments consist in two main sections: the riser, where the air is sparged and the liquid flows up and, the down comer, where the liquid flows down. These sections are connected by the gas-liquid separator, at the top of the bioreactor, and by the base, at the bottom of the equipment.

The hydrodynamic of airlift bioreactors is strongly related to their geometry, exhibiting a complex relationship between operation/design variables and performance parameters [4]. The design variables include the reactor height, the downcomer-to-riser cross sectional area ratio (A_D/A_R), gas-liquid separator geometry and, bottom clearance. In spite of the developments in recent years, the relationship between these geometrical variables and performance parameters remain still unclear, for proper design and scale-up purposes [1], [4].

The gas-liquid separator is an important section of airlift bioreactors since it promotes the gas disengagement and liquid

recirculation, and its geometry affects the gas hold-up and liquid circulation velocity [4], [5], which govern the oxygen mass transfer from the gas to the liquid phase [6]. Studies on this field investigated the influence of liquid volume present in this region [6]-[9], the presence of an expanded gas-liquid separator [8], [10], and the diameter of the expansion [7], [8] on the performance of concentric-tube airlift bioreactors (*CTAB*). However, these studies analyzed each variable independently without consider the possible interactions between them in order to define the best geometry.

The aim of this study was to define the best gas-liquid separator geometry of a *CTAB*, evaluating the influence of the liquid volume fraction on the gas-liquid separator (V_{GLS}), the gas-liquid separator openness angle (α), and the specific air flow rate (ϕ_{AIR}) on hydrodynamics and oxygen transfer, using response surface methodology.

II. MATERIALS AND METHODS

A. Bioreactors

The experiments were carried out in 10-L concentric-tube airlift bioreactors (made in acrylic) with reversed conical gas-liquid separator (Fig. 1), whose openness angle varied from 30 to 90° and the liquid volumetric fraction varied from 10 to 30%, comprising ten different bioreactor configurations. The column diameter was 16.0cm and the draft tube diameter was 10.0cm, giving a downcomer-to-riser cross sectional area ratio of 1.56.

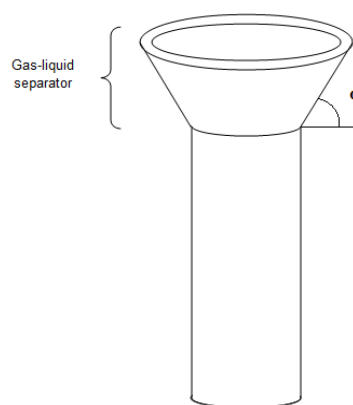


Fig. 1 Scheme of an airlift bioreactor with enlarged gas separator

The system were equipped with a gas flow meter (Aalborg model GFC37), dissolved oxygen analyzer (Mettler Toledo O₂ Transmitter 4500) and probe (Mettler Toledo InPro 6100), and a data acquisition system to enable measurements of dissolved oxygen concentration in real time.

M. N. Esperança is with the Department of Chemical Engineering, Federal University of São Carlos, São Carlos, SP, Brazil (e-mail: mateus.nordi@gmail.com).

M. O. Cerri is with Department of Chemistry, Biotechnology and Bioprocess Engineering, Federal University of São João Del-Rey, Ouro Branco, MG, Brazil (e-mail: marcelcerri@ufsj.edu.br).

A. C. Badino is with the Department of Chemical Engineering, Federal University of São Carlos, São Carlos, SP, Brazil (phone: 55 16 3351-8001 ; fax: 55 16 3351-8266 ; e-mail: badinojr@ufscar.br).

B. Fluids

Distilled water was used as Newtonian fluid and a xanthan gum solution (2.5g.L^{-1}) supplemented with 10g.L^{-1} of steam exploded sugarcane bagasse with particle diameter inferior to 1.0mm was used as pseudoplastic fluid in order to simulate non-Newtonian fermentation broth involving filamentous microorganism. The dynamic viscosity of distilled water ($\mu = 8.4 \cdot 10^{-4} \text{ Pa.s}$) and power law model rheological parameters for xanthan gum solution (consistency index, $K = 1.01 \text{ Pa.s}^n$, and the flow index, $n = 0.28$) were determined from rheograms using a digital concentric-cylinder rheometer (Brookfield Engineering Laboratories), model DVIII Ultra at 32°C .

C. Experimental Design and Statistical Analysis

A full factorial design was used to evaluate the effects of specific airflow rate (ϕ_{AIR}), gas-liquid separator openness angle (α), and liquid volumetric fraction on the gas-liquid separator (V_{GLS}) on response variables volumetric oxygen transfer coefficient ($k_L a$) and global gas hold-up (ε_G). The full 2^3 factorial design comprises eight factorial points, six axial points and three central points, with the experiments carried out in random order [11]. Table I presents the codified and real values for independent variables. A statistical software package (Statsoft v. 7.0) was used to analyze the experimental data, generate ANOVA (analysis of variance) results and obtain the response surfaces.

TABLE I
CODIFIED AND REAL VALUES OF INDEPENDENT VARIABLES

Levels	Variable		
	α ($^\circ$)	V_{GLS} (-)	ϕ_{AIR} (vvm ^a)
-1.68	30	0.10	1.0
-1	42	0.14	1.8
0	60	0.20	3.0
1	78	0.26	4.2
1.68	90	0.30	5.0

^aThe unit vvm corresponds to volume of gas per volume of aerated liquid per minute.

D. Determination of Volumetric Oxygen Transfer Coefficient ($k_L a$)

The volumetric oxygen transfer coefficient was determined using the dynamic method [12], considering the first-order probe-delay response [13]. This method consists in monitor the dissolved oxygen concentration in the fluid using an oxygen sensor. Initially, the sensor located in the riser section of airlift bioreactor was calibrated under O_2 saturation conditions. In the sequence, all dissolved oxygen (DO) of the system was removed by N_2 bubbling into the vessel. Then, a constant airflow rate was supplied into the bioreactor with simultaneous and continuous measurements of DO concentration until the saturation be reached. Model giving by (1) was fitted to DO concentration data, obtaining $k_L a$ values.

$$C = C_{e0} \cdot e^{-k_e(t-t_0)} + C_{es} \cdot (1 - e^{-k_e(t-t_0)}) + \frac{k_e(C_{es} - C_0)}{k_e - k_L a} (e^{-k_e(t-t_0)} - e^{-k_L a(t-t_0)}) \quad (1)$$

where C_{e0} is the DO concentration value read by the sensor in the beginning of air supply, C_{es} is the saturation DO concentration read by the probe, and k_e is the electrode delay constant, defined as the inverse of sensor response time (τ_e).

E. Determination of Gas Hold-Up (ε_G)

The global gas hold-up was determined by the volume expansion technique [12]. This method consists in visual measurements of gas-liquid dispersion height (h_D) under aeration and non-aerated liquid height (h_L). Global gas hold-up was calculated by (2):

$$\varepsilon_G = \frac{h_D - h_L}{h_D} \quad (2)$$

III. RESULTS AND DISCUSSION

The global gas hold-up (ε_G) and the volumetric oxygen transfer coefficient ($k_L a$) are important parameters in pneumatic bioreactors. Therefore, for each fluid a set of two 2^3 full factorial designs were used to evaluate the effects of specific airflow rate (ϕ_{AIR}), gas-liquid separator openness angle (α) and, liquid volumetric fraction on the gas-liquid separator (V_{GLS}) on $k_L a$ and ε_G .

A. Newtonian Fluid

Table II presents the results of $k_L a$ and ε_G as function of independent variables ϕ_{AIR} , α and, V_{GLS} for distilled water.

Using the Statsoft software, $k_L a$ and ε_G data were fitted to a second-order polynomial model in order to verify the statistically significant terms and exclude the non-significant ones. The $k_L a$ and ε_G models were submitted to an analysis of variance (ANOVA) which yielded F-values 25.0 and 10.2-fold higher than the tabled F-values, respectively, at a 90% confidence level. These results were considered satisfactory to use the models (3) and (4) for prediction, in which x_1 , x_2 , and x_3 are the coded variables for gas-liquid separator openness angle (α), liquid volumetric fraction on the gas-liquid separator (V_{GLS}), and specific airflow rate (ϕ_{AIR}), respectively.

$$k_L a \cdot 10^2 = 4.7 + 0.43 \cdot x_1 + 0.21 \cdot x_1^2 - 0.34 \cdot x_2 + 1.08 \cdot x_3 - 0.42 \cdot x_3^2 \quad (3)$$

$$\varepsilon_G \cdot 10^2 = 8.7 - 1.7 \cdot x_1 - 2.0 \cdot x_2 - 1.5 \cdot x_2^2 + 2.2 \cdot x_3 + 1.0 \cdot x_1 \cdot x_2 \quad (4)$$

Comparing constant values in (3), it can be observed that linear term of the specific airflow rate (x_3) contributed with the major influence on oxygen mass transfer, since its coefficient (1.08) was one magnitude-order higher than the other constants.

TABLE II
VOLUMETRIC OXYGEN TRANSFER COEFFICIENT AND GLOBAL GAS HOLD-UP
FOR CTAB OPERATING WITH DISTILLED WATER

Assay	α (°)	V_{GLS} (-)	Φ_{AIR} (vvm)	$k_L a$ (s ⁻¹)	ϵ_G (-)
1	42	0.14	1.8	0.0306	0.1010
2	78	0.14	1.8	0.0387	0.0446
3	42	0.26	1.8	0.0268	0.0277
4	78	0.26	1.8	0.0288	0.0229
5	42	0.14	4.2	0.0556	0.1435
6	78	0.14	4.2	0.0629	0.0833
7	42	0.26	4.2	0.0435	0.0714
8	78	0.26	4.2	0.0473	0.0408
9	30	0.20	3.0	0.0461	0.1160
10	90	0.20	3.0	0.0683	0.0713
11	60	0.10	3.0	0.0505	0.0709
12	60	0.30	3.0	0.0474	0.0353
13	60	0.20	1.0	0.0208	0.0566
14	60	0.20	5.0	0.0581	0.1490
15	60	0.20	3.0	0.0443	0.0929
16	60	0.20	3.0	0.0495	0.0885
17	60	0.20	3.0	0.0498	0.0639

In order to define the better gas-liquid separator geometry, it was defined an operational condition of 3.0 vvm ($x_3 = 0$), which represents an usual value in bioprocess applications. Using the Statsoft software, the contour plots for $k_L a$ and ϵ_G represented by Figs. 2 and 3, were obtained.

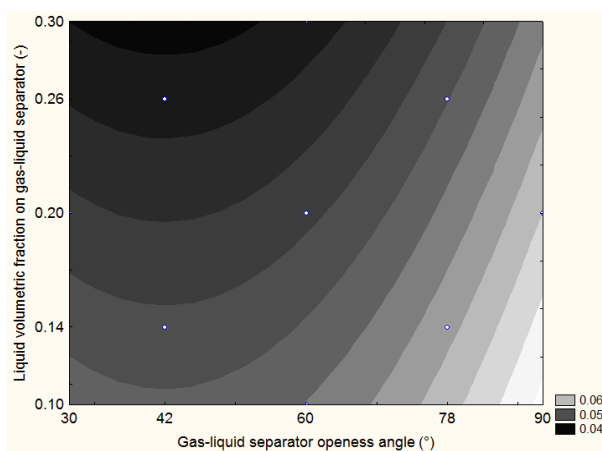


Fig. 2 Contour plot for $k_L a$ at $\Phi_{AIR} = 3$ vvm operating with distilled water

According to Fig. 2, an increment in oxygen mass transfer (represented by $k_L a$ value) was achieved increasing α and decreasing V_{GLS} . Similar behavior was observed in studies using water-in-oil microemulsion [8] and water [14], in different scales of concentric-tube airlift bioreactors (30 and 300-L) with different downcomer-to-riser cross sectional area ratio (0.707-1.306).

In the opposite way, an improvement in global gas hold-up (ϵ_G) occurred with decreasing both α and V_{GLS} (Fig. 3). A reduction in the liquid volumetric fraction on gas-liquid separator provides a shorter fluid residence time in gas-liquid separator, which allows a higher gas recirculation, and

consequently, a higher gas hold-up [14].

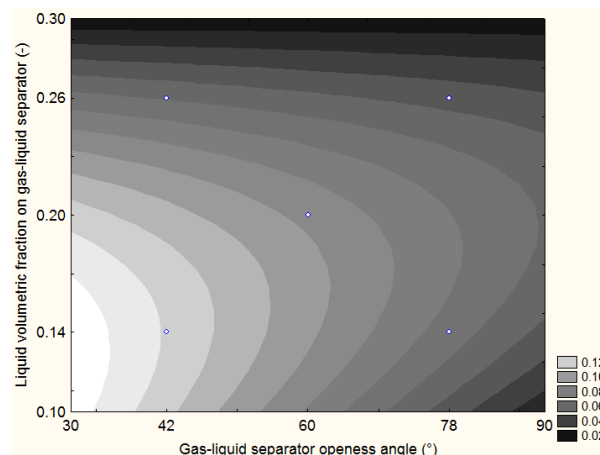


Fig. 3 Contour plot for ϵ_G at $\Phi_{AIR} = 3$ vvm operating with distilled water

Analyzing Fig. 2, the best gas-liquid separator geometry presented an openness angle of 90° and a liquid volumetric fraction of 10%. This design combined the highest $k_L a$ value of the system (0.06 s⁻¹) with the lowest global gas hold-up (0.02), which indicates that even for a small amount of bubbles retained in the liquid phase, the oxygen transfer was high. This behavior can be explained by a decrease in the gas bubble diameter (d_B), which increased the specific interfacial area (a) for oxygen transfer, and consequently, the $k_L a$ value.

B. Non-Newtonian Fluid

Table III presents the results of $k_L a$ and ϵ_G for xanthan gum solution supplemented with steam exploded sugarcane bagasse.

TABLE III
VOLUMETRIC OXYGEN TRANSFER COEFFICIENT AND GLOBAL GAS HOLD-UP
FOR CTAB OPERATING WITH NON-NEWTONIAN FLUID

Assay	α (°)	V_{GLS} (-)	Φ_{AIR} (vvm)	$k_L a$ (s ⁻¹)	ϵ_G (-)
1	42	0.14	1.8	0.0053	0.0366
2	78	0.14	1.8	0.0055	0.0464
3	42	0.26	1.8	0.0052	0.0484
4	78	0.26	1.8	0.0051	0.0397
5	42	0.14	4.2	0.0109	0.0827
6	78	0.14	4.2	0.0127	0.1135
7	42	0.26	4.2	0.0112	0.0254
8	78	0.26	4.2	0.0129	0.0830
9	30	0.20	3.0	0.0079	0.2153
10	90	0.20	3.0	0.0097	0.0832
11	60	0.10	3.0	0.0101	0.0686
12	60	0.30	3.0	0.0080	0.0952
13	60	0.20	1.0	0.0034	0.0624
14	60	0.20	5.0	0.0162	0.1304
15	60	0.20	3.0	0.0076	0.0813
16	60	0.20	3.0	0.0099	0.0958
17	60	0.20	3.0	0.0088	0.0886

Following the same procedure used in distilled water data, ANOVA was applied to (5) and (6) with the non-significant terms already excluded. F-values were 63.1 and 2.5-fold higher than the tabled F-values, respectively, at a 90% confidence level.

$$k_L a \cdot 10^3 = 8.8 + 0.5 \cdot x_1 - 0.3 \cdot x_2 + 3.5 \cdot x_3 + 0.4 \cdot x_1 \cdot x_3 \quad (5)$$

$$\varepsilon_G \cdot 10^2 = 9.3 - 1.4 \cdot x_2^2 + 1.8 \cdot x_3 \quad (6)$$

As well as distilled water data, linear specific airflow rate (x_3) played the highest influence on oxygen mass transfer for non-Newtonian fluid, as can be seen in (5). In this system, $k_L a$ was one-magnitude order lower than the observed for distilled water system.

Fixing the specific airflow rate at 3.0 vvm ($x_3 = 0$), the contour plots for $k_L a$ (Fig. 4) and ε_G (Fig. 5) were obtained using the Statsoft software.

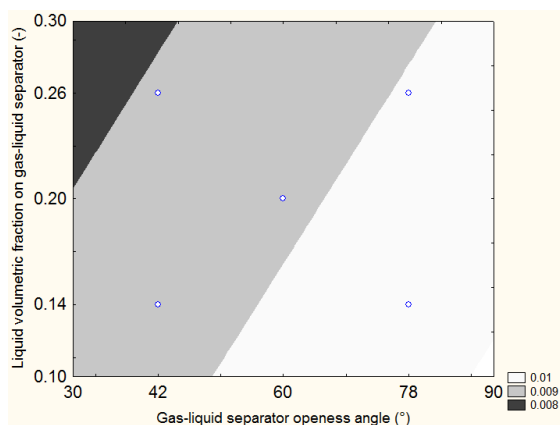


Fig. 4 Contour plot for $k_L a$ at $\Phi_{AIR} = 3$ vvm operating with non-Newtonian fluid

Following the same trend observed in Newtonian fluid (water), an increment in α and reduction in V_{GLS} promoted an improvement in oxygen mass transfer for xantham gum solution. However, for non-Newtonian fluid, these effects were less pronounced than in water. In this case, the higher $k_L a$ value could be obtained for α ranging from 60° to 90° and V_{GLS} varying from 10 to 30% (Fig. 4), allowing different geometries in gas-liquid separator.

According to Fig. 5, global gas hold-up was not affected by α , operating at 3.0 vvm. In the other hand, V_{GLS} played an important role, determining the highest value of gas hold-up for 20% of liquid present in gas-liquid separator.

The best gas-liquid separator design for non-Newtonian fluid correspond to a liquid volumetric fraction of 10% and an openness angle varying from 60° to 90°. This geometry comprises the highest volumetric oxygen transfer coefficient ($k_L a = 0.01 \text{ s}^{-1}$) for xantham gum solution, and the lowest gas hold-up (0.06). Taking into account the bioreactor construction, however, the best gas-liquid separator presents a 90° openness angle.

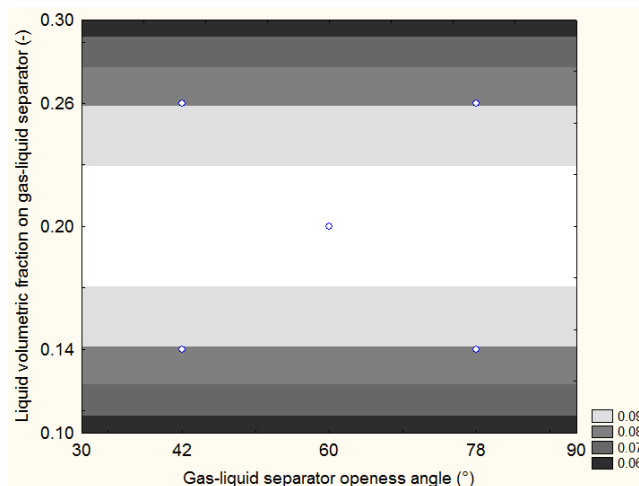


Fig. 5 Contour plot for ε_G at $\Phi_{AIR} = 3$ vvm operating with non-Newtonian fluid

IV. CONCLUSIONS

Specific airflow rate exerted the higher influence on oxygen mass transfer for both Newtonian and non-Newtonian fluids. While the openness angle of gas-liquid separator and the specific airflow rate affected positively the oxygen mass transfer ($k_L a$), the liquid volumetric fraction in the gas-liquid separator exhibited a negative effect. For distilled water, the geometric variables affected negatively the global gas hold-up (ε_G), while for xantham gum solutions the openness angle presented no effect. The best geometry of the gas-liquid separator corresponds to a 90° openness angle and 10% of liquid in the degassing zone. This design comprises the higher $k_L a$ for the systems with the lower ε_G .

ACKNOWLEDGMENT

The authors are grateful for the financial supports provided by Human Resources Program of Agência Nacional de Petróleo, Gás Natural e Biocombustíveis, Brazil (PRH/ANP) and Fundação de Amparo à Pesquisa do Estado de São Paulo, Brazil (FAPESP, Proc 2011/23807-1).

REFERENCES

- [1] P. M. Kilonzo, A. Margaritis, M. A. Bergougno, J. Yu, Y. Qin, "Effects of geometrical design on hydrodynamics and mass transfer characteristics of a rectangular-column airlift bioreactor", *Biochem Eng J*, vol. 34, pp. 279-288, 2007.
- [2] Y. Wei, W. Tiefeng, L. Malin, W. Zhanwen, "Bubble circulation regimes in a multi-stage internal-loop airlift reactor", *Chem Eng Sci*, vol. 142, pp. 301-308, 2008.
- [3] M. O. Cerri, A. C. Badino, "Oxygen transfer in three scales of concentric tube airlift bioreactors", *Biochem Eng Sci*, vol. 51, pp. 40-47, 2010.
- [4] J. C. Merchuk, N. Ladwa, A. Cameron, M. Bulmer, I. Berzin, A. M. Pickett, "Liquid flow and mixing in concentric tube air-lift reactors", *J Chem Tech Biotech*, vol. 66, pp. 174-182, 1996.
- [5] F. Gumery, F. Ein-Mozaffari, Y. Dahan, "Characteristics of local flow dynamics and macro-mixing in airlift column reactors for reliable design and scale-up", *Int J Chem React Eng*, vol. 7, 2009.
- [6] P. M. Kilonzo, A. Margaritis, M. A. Bergougno, J. Yu, Y. Qin, "Influence of the baffle clearance design on hydrodynamics of a two-riser rectangular airlift reactor with inverse internal loop and expanded gas-liquid separator", *Chem Eng J*, vol. 121, pp. 17-26, 2006.

- [7] M. R. Mehrnia, B. Bonakdarpour, J. Towfighi, M. M. Akbarnejad, "Design and operational aspects of airlift bioreactors for petroleum biodesulfurization", *Environmental Progress*, vol. 23, n. 3, pp. 206-214, 2004.
- [8] M. R. Mehrnia, J. Towfighi, B. Bonakdarpour, M. M. Akbarnejad, "Influence of top-section design and draft tube height on the performance of airlift bioreactors containing water-in-oil microemulsion", *J Chem tech Biotech*, vol. 79, pp. 260-267, 2004.
- [9] J. Klein, A. A. Vicente, J. A. Teixeira, "Hydrodynamics of a three-phase airlift reactor with an enlarged separator – Application to high cell density systems", *Canadian J Chem Eng*, vol. 81, pp. 433-443, 2003.
- [10] J. Klein, S. Godos, O. Dolgos, J. Markos, "Effect of a gas-liquid separator on the hydrodynamics and circulation flow regimes in internal-loop airlift reactors", *J Chem Tech Biotech*, vol. 76, pp. 516-524, 2001.
- [11] D. C. Montgomery, *Design and Analysis of Experiments*. New York, 2001.
- [12] Y. Chisti, *Airlift bioreactors*. Belfast, Elsevier Science Publishers Ltd., 1989.
- [13] S. Aiba, A.E. Humphrey, F. Millis, *Biochemical Engineering*. Tokyo, University of Tokyo Press, 1973.
- [14] J. C. Merchuk, N. Ladwa, A. Cameron, M. Bulmer, A. M. Pickett, "Concentric tube airlift reactors: effects of geometrical design on performance", *AIChE J*, vol. 40, n. 7, pp. 1105-1117, 1994.